Control of Complex Dynamics with Time-Delayed Feedback in Populations of Chemical Oscillators: Desynchronization and Clustering

Yumei Zhai, István Z. Kiss, and John L. Hudson*

Department of Chemical Engineering, 102 Engineers' Way, University of Virginia, Charlottesville, Virginia 22904-4741

Control of collective dynamics with global time-delayed feedback was experimentally studied with (phase) synchronized populations of smooth, relaxational, and chaotic electrochemical oscillators. The experimental results provide laboratory evidence for the findings in the studies of delayed feedback on phase oscillators; multiple, isolated regions of desynchronization in the parameter plane, hysteresis phenomenon around the boundaries of control regions, synchronization of irregular behavior with very strong feedback strength, and a shift of the synchronization transition curves were reproduced in experiments. In addition, it is observed that clustering accompanies the occurrence of desynchronization in delayed feedback of relaxational oscillators. For populations of elements that are close to Hopf bifurcation, desynchronization, amplitude death, and enhanced synchronization occurs with a low, intermediate, and high delay time, respectively.

1. Introduction

Spatiotemporal patterns can occur in dissipative distributed chemically reacting systems;[1,2] the interaction of nonlinear reaction and coupling among reaction sites determines the structure, and such structures can be controlled and engineered through external signals (pacemakers), feedback, and patterned catalytic structure.[3−11] Nonstationary reaction rates and their nontrivial spatial dependence produces many interesting phenomena including moving hot spots,[12] traveling reaction waves,[13] and spirals.[14] The control of the characteristic features of the self-organized structure of such systems requires mild inputs that do not destroy the qualitative underlying dynamics of the local behavior.[4]

The collective dynamics of large sets of coupled discrete oscillators encompasses a variety of possible spatiotemporal phenomena, including desynchronization, clustering/pattern formation, amplitude death, and synchronization.[15−18] Global time-delayed feedback has been studied as an effective way to tune the collective dynamics of an oscillator population in theories,[19,20] simulations,[19−25] and experiments.[11,25−28] The feedback can be applied to a population to stabilize otherwise unstable solutions or produce new states. This method is convenient, because (i) a global control eliminates the need of the access to all local elements and (ii) the feedback does not require extensive real-time computations. In addition, in feedback methods, an acting force is generated by the system itself and therefore automatically adjusts to the variations of the system states, which can be very useful in demand-controlled applications.

Global feedback has been investigated in extended systems. Suppression of spatiotemporal chaos by forming periodic clusters or a homogeneous state are found in global delayed feedback on a weakly diffusive coupled logistic map lattice[22] and on a diffusively coupled complex Ginzburg−Landau equation.[21] In experiments, various spatiotemporal patterns in the catalytic CO oxidation on Pt(110)[11] and oscillatory cluster patterns in a Belousov−Zhabotinsky reaction−diffusion system[26] were produced with global delayed feedback. Previous studies[27−29] on global feedback on a chaotic electrochemical oscillator population with intermediate coupling showed that intermittent clusters, stable chaotic clusters, periodic clusters (the periodicity decrease with feedback gain), stable synchronized period-1 and steady state are obtained as the gain increases.

Recently, desynchronization with time-delayed feedback has received attention, because of its possible application in medical treatment of some diseases associated with pathological synchronization of neurons. Rosenblum and Pikovsky[19,20] proposed linear time-delayed feedback for effective desynchronization of a synchronized oscillator population. They demonstrated numerically and theoretically that there exist bounded regions of desynchronization and enhanced synchronized in the parameter plane of feedback gain and time delay. The results of their theoretical analysis also show that there are bistability regions near the boundaries of each desynchronization control region in which either desynchronized or synchronized state can be stable. With very strong feedback gain, the uniformly rotating state is no longer stable. Hauptmann, Popovych, and Tass[24] studied a spatially coordinated time-delayed feedback on modeled networks of coupled neurons as a robust and mild technique for desynchronization. The same group later developed a nonlinear feedback method[25] with which no enhanced synchronized regions coexist with the desynchronization regions in the parameter plane.

However, the comprehensive understanding of global time-delayed feedback control of a synchronized population is lacking, especially from the experimental standpoint. In this work, we apply various global linear time-delayed feedback schemes on a (phase) synchronized population of smooth, relaxational, and chaotic electrochemical oscillators and study how the feedback destroys, enhances, or modifies the underlying collective dynamics.

2. Experimental Setup and Methods

The experiments were performed using an array of electrodes, as shown in Figure 1. A standard electrochemical cell consisting of a nickel working electrode array (64 1-mm diameter electrodes with an 8×8 configuration), a Hg/Hg_2SO_4 reference electrode, and a platinum mesh counterelectrode was used.

* To whom correspondence should be addressed. Tel.: +1-434-924-6275. Fax: +1-434-982-2658. E-mail address: hudson@virginia.edu.

10.1021/ie0708632 CCC: $40.75
Published on Web 12/05/2007

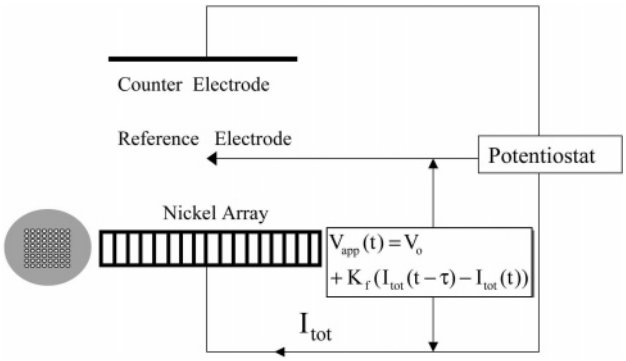

Figure 1. Schematic of an apparatus with feedback. In this example, the feedback term is given as $\delta V = K_f(I_{tot}(t - \tau) - I_{tot}(t))$.

Experiments were conducted in a sulfuric acid solution at a temperature of 11 °C. The working electrodes are embedded in epoxy, and reaction occurs only at the ends. A constant potential (V_0 versus the reference electrode) is applied to all electrodes through a potentiostat. The feedback signal (δV) is superimposed to V_0 via the potentiostat. Real-time Labview was used to visualize and save the individual current data on a computer, as well as to generate and emit a feedback signal to the potentiostat. The sampling rate was 100 Hz. Because the currents of all the individual electrodes are measured, the rate of reaction, as a function of position and time, is obtained.

The electrodes were connected to the potentiostat through 64 uniform individual resistors that were connected to each of the electrodes (R_{ind}) and one collective resistor (R_{coll}) (not shown in the figure). The collective resistor couples the electrodes globally.[30,31] We used a method of altering the strength of global coupling while holding other parameters constant,[31] in which the total external resistance ($R_{tot} = R_{coll} + R_{ind}/N$) was held constant while the fraction that was dedicated to individual currents, as opposed to the total current, was varied. A global coupling parameter, defined as $\epsilon = R_{coll}/R_{tot}$, takes on values from 0 for the case where no global coupling occurred to 1 for the strongest added global coupling case. The coupling among the electrodes occurs through the electrode potentials, and the following set of ordinary differential equations (ODEs) was derived[32] to describe the electrode potential of the electrodes (e_k, where $k = 1, 2, ..., N$) of the coupled metal dissolution system:

$$\frac{de_k}{dt} = \frac{V_0 - e_k}{NR_{tot}} - i_F(e_k,\theta_k) + \frac{K}{NR_{tot}}(\langle e\rangle - e_k)$$

where i_F is the Faradaic current, which is dependent on the electrode potential and the surface coverage of NiO and NiOH species. The effect of the coupling can be seen in the appearance of a coupling term that contains the mean electrode potential $\langle e\rangle$ in the charge balance equation.

When the electrolyte concentration was 3 mol/L H_2SO_4 and the total resistance was 10.2 Ω, the current of a single electrode underwent a Hopf bifurcation at $V_0 \cong 1.05$ V to be oscillatory as the applied potential increased. At a potential above and near the Hopf bifurcation point, the angular velocity of the oscillations was almost constant and we refer to these oscillations as smooth. The oscillations ceased at $V_0 \cong 1.30$V with a saddle-loop bifurcation, below which there was a region of relaxation oscillations where the angular velocity varied with time. In a 4.5 mol/L H_2SO_4 solution with a total resistance of 14.2 Ω, Hopf and saddle-loop bifurcation occurred, at $V_0 \cong 1.26$ V and $V_0 \cong 1.63$ V, respectively. Near the Hopf bifurcation point, there was a window of circuit potential ($V_0 \cong 1.285-1.400$ V) within which chaotic oscillations were observed.

A (nearly) phase-synchronized state was obtained at the beginning of the experiments by increasing the global coupling strength among the population. Various global feedback schemes were implemented with Real-Time Labview to study the effects of time-delayed feedback on the dynamics of the cluster.

When clustering occurs, the population of oscillators can be classified into groups of elements (clusters) within which the experimental observables (e.g., current) are synchronized (i.e., vary identically with time). The behavior of the elements, however, is different from those of the elements in the other clusters. At selected times N (here, $N = 100 \times T_0$, where T_0 is the period of the mean current), the three state space coordinates of each element are recorded. The jth observation of the kth element is $\mathbf{x}_{j,k}$, where $\mathbf{x}_{j,k}$ is a three-dimensional vector ($j = 1, ..., N$, $k = 1, ..., 64$). The distances ($\delta_{k,l}$) among the observation vectors ($\mathbf{X}_k = \{\mathbf{x}_{1,k}, \mathbf{x}_{2,k}, ..., \mathbf{x}_{N,k}\}$) of each pair of elements in the $N \times 3$ dimensional space are determined ($\delta_{k,l} = |\mathbf{X}_k - \mathbf{X}_l|$) and a cluster tree is constructed using an average distance algorithm. Element k is classified to belong to a cluster of the set of elements with precision E if $|\mathbf{X}_k - \bar{\mathbf{X}}| < E$, where $\bar{\mathbf{X}}$ is the mean value of observation vectors of the cluster. Each line at a precision E in a cluster tree (such as that shown below in Figure 9d) identifies a cluster; the number of lines at a given clustering distance (E) shows the number of clusters to a value within that precision; in addition, the elements belonging to a certain cluster (one vertical line) can be obtained by following the branch. We used $E = 0.2$ in this paper.

3. Time-Delayed Feedback Schemes

Four different feedback schemes for the feedback terms δV were used in this study.

The feedback can be simply based on the total current, which is a measurable quantity. In direct time-delayed feedback of the total current, the feedback term is expressed as

$$\delta V(t) = K_f I_{tot}(t - \tau) \tag{1}$$

where the time delay τ is defined as the ratio of the time delay (given in seconds) to the period T_0 (also given in seconds). The voltage perturbation expressed in eq 1 will not have a mean value of 0 if $\langle I_{tot}\rangle \neq 0$; this may substantially deviate the individual dynamics from those without feedback if the feedback strength is large. To remove the effects of nonzero $\langle \delta V\rangle$ in experiments, a previously calculated mean perturbation was subtracted from the right-hand side of eq 1, i.e.,

$$\delta V(t) = K_f I_{tot}(t - \tau) - \langle \delta V\rangle_{preset} \tag{2}$$

Another way to avoid the nonzero $\langle \delta V\rangle$ problem is to use differential time-delayed feedback of the total current,

$$\delta V(t) = K_f[I_{tot}(t - \tau) - I_{tot}(t)] \tag{3}$$

However, the dynamical variable of this system, i.e., that which appears in the governing ODE model, is the potential drop through the double layer of the electrode.[33,34] Thus, the mean field of this system is the mean potential drop (e_{mean}). From the analysis of the equivalent circuit of the experimental system,[32] we obtain the relationship between e_{mean} and I_{tot} as

$$I_{tot} = \frac{1}{R_{tot}}(V_0 + \delta V - e_{mean}) \tag{4}$$

We also implemented time-delayed feedback based on the mean potential drop. In the direct time-delayed feedback of e_{mean}, the perturbation term δV is expressed as

$$\delta V(t) = -\left(\frac{K_f}{R_{tot}}\right) e_{mean}(t-\tau) \quad (5)$$

The value $e_{mean}(t-\tau)$ cannot be directly measured in the experiments; therefore, we rewrite eq 5 as a function of $I_{tot}(t-\tau)$, with the help of eq 4:

$$\delta V(t) = K_f\left[I_{tot}(t-\tau) - \frac{V_0 + \delta V(t-\tau)}{R_{tot}}\right] \quad (6)$$

Now all quantities ($I_{tot}(t-\tau)$ and $\delta V(t-\tau)$) on the right-hand side of eq 6 are measurable; this recursive feedback formula ensures that the feedback term is proportional to the dynamical variable (i.e., the mean potential drop e_{mean}). Note that the feedback strength or gain is controlled by parameter K_f in the experiments, although the real feedback strength in eq 5 is given as

$$K_f' = -\frac{K_f}{R_{tot}}$$

Similar to the direct time-delayed feedback of the total current, the direct feedback of e_{mean} may also have the problem of changing the individual dynamics because of a nonzero mean value of $\delta V(t)$ (if $\langle e_{mean}\rangle \neq 0$). Therefore, again, in the experiments, the mean value of $\delta V(t)$ was monitored before imposition of the feedback signal to obtain a precalculated mean δV and then a compensation was made such that $\delta V(t)$ was almost zero by subtracting the feedback signal with $\langle \delta V\rangle_{preset}$:

$$\delta V(t) = K_f\left[I_{tot}(t-\tau) - \frac{V_0 + \delta V(t-\tau)}{R_{tot}}\right] - \langle \delta V\rangle_{preset} \quad (7)$$

In differential feedback of the mean potential drop, the perturbation term is expressed as

$$\delta V(t) = -\left(\frac{K_f}{R_{tot}}\right)[e_{mean}(t-\tau) - e_{mean}(t)] \quad (8)$$

With the help of eq 4, the perturbation term can be rewritten with $I_{tot}(t-\tau)$ and $\delta V(t-\tau)$ as

$$\delta V(t) = K_f\left\{[I_{tot}(t-\tau) - I_{tot}(t)] + \left[\frac{\delta V(t-\tau) - \delta V(t)}{R_{tot}}\right]\right\} \quad (9)$$

Because of the appearance of $\delta V(t)$ on the both sides of eq 9, we treated the $\delta V(t)$ on the right-hand side as $\delta V(t-\tau_0)$, where $\tau_0 = 0.01$ s is the smallest time delay that the controller can attain. Note that, with this feedback scheme, the actual feedback strength in eq 8 is again $K_f' = -K_f/R_{tot}$.

There is another way to implement the differential mean-field time-delayed feedback which can avoid the appearance of $\delta V(t)$ on the both sides of the expression of the perturbation term. If we let

$$\delta V(t) = \left[-\left(\frac{K_f}{R_{tot} + K_f}\right)\right][e_{mean}(t-\tau) - e_{mean}(t)] \quad (10)$$

then the perturbation, in terms of $I_{tot}(t-\tau)$ and $\delta V(t-\tau)$, will be

$$\delta V(t) = K_f\left\{[I_{tot}(t-\tau) - I_{tot}(t)] - \frac{\delta V(t-\tau)}{R_{tot}}\right\} \quad (11)$$

We implemented both eqs 9 and 11 in the experiments, and no noticeable difference in the results was observed.

For better direct comparison with theory,[19] we define the feedback strength K_f' for the dynamical variable e_{mean} as

$$K_f' = -K_f$$

4. Feedback on Populations of Smooth Oscillators: Desynchronization and (Enhanced) Synchronization of Periodic and Irregular Behavior

4.1. Direct Feedback of Total Current. We first applied direct time-delayed feedback of the total current (eq 2) to a phase-synchronized population of 64 smooth electrochemical oscillators.

Effective desynchronization occurs with appropriate K_f' and τ. A typical experimental result of desynchronization by time-delayed feedback is illustrated in Figure 2, where $K_f' = -2.5$ and $\tau = 0.005$. Before the application of the feedback (at the time earlier than the left arrow in Figure 2a), the population was highly synchronized; the collective signal (the mean current) exhibited large oscillations, with amplitudes comparable to those of the individual currents (Figure 2a). The amplitudes of the mean current started to decrease when the feedback was turned on while the individual currents maintained original oscillations. The oscillation of the mean current almost vanished after ~10 cycles. Simultaneously, the feedback signal decreased to almost zero after the mean current attained an almost steady state. However, this very small magnitude of the feedback signal has an important role in stabilizing the incoherent state. After the feedback was removed, as also shown in Figure 2a at the time later than the right arrow, the collective signal restarted oscillations with increasing amplitudes. The behavior of all 64 oscillators in the feedback experiment can be observed from the grayscale plot of individual currents in Figure 2b. The imposition of the feedback at $t \approx 10$ s broke up the uniform dynamics and all elements maintained periodic oscillations but the phases were no longer locked during the feedback.

The phase dynamics of all 64 elements can be better seen in a two-dimensional (2D) phase space. We constructed the phase space using the Hilbert transform,

$$h(x(t)) = \frac{1}{\pi} PV \int_{-\infty}^{\infty} \frac{x(t)}{t-\tau}\, d\tau$$

of the individual current,[35,36] $h[I(t) - \langle I\rangle]$. (The phase space reconstruction with the Hilbert transform is analogous to the reconstruction using delay coordinates; however, it does not require the use of a delay time.) The points on a snapshot in the quantity $(I(t) - \langle I\rangle)$ versus h space at $t = 69$ s (during the feedback) were fairly well-distributed on the limit cycle (Figure 2c), which indicates that an effective desynchronization was obtained with the feedback.

An order parameter similar to the Kuramoto order[32] is defined as

$$r = \frac{\left|\sum_j \mathbf{P}_j(t)\right|}{\sum_j |\mathbf{P}_j(t)|} \quad (12)$$

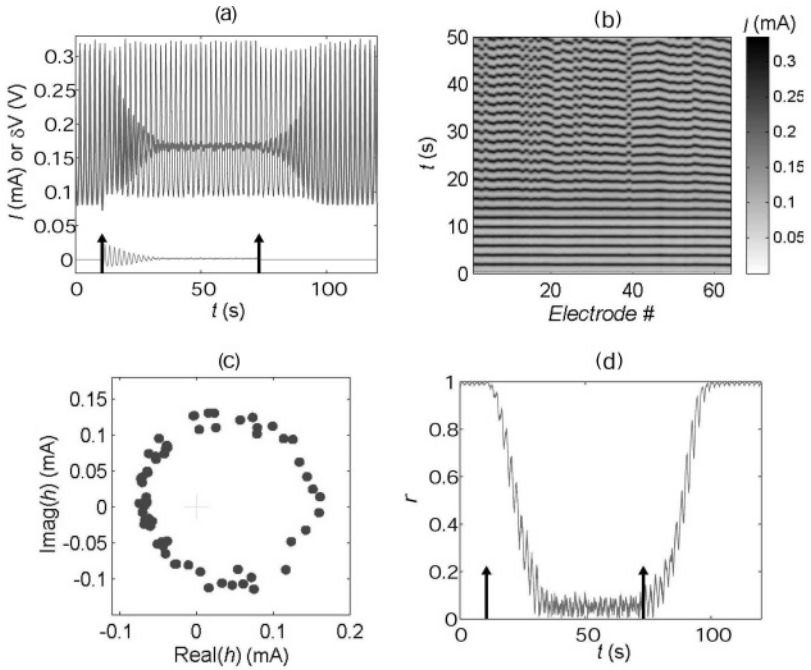

Figure 2. Desynchronization of a population of smooth electrochemical oscillators with direct time-delayed feedback of the total current (I_{tot}); parameter values are $c = 3$ mol/L, $R_{tot} = 10.2\ \Omega$,$V_0 = 1.123$ V, and $\epsilon = 0.2$. The left column shows data for a feedback strength of $K_f' = -2.5$ and time delay of $\tau = 0.005$; the right column shows data for $K_f' = -3$ and $\tau = 0.031$. (a) Time series of mean current (bold line), individual current (thin line), and feedback signal; arrows indicate the beginning and end of the feedback procedure. (b) Grayscale plot of individual currents. (The elements are ordered by their intrinsic frequencies from low to high.) (c) Snapshot of phase points during the feedback ($t = 69$ s) in the two-dimensional (2D) phase space constructed with a Hilbert transform of the currents. (d) Time series of order r; the mean order $\langle r \rangle$ decreased from 0.992 to 0.054, because of the feedback (obtained by averaging for 40 s after the transition). For smooth populations, $T_0 \approx 1.95$ s.

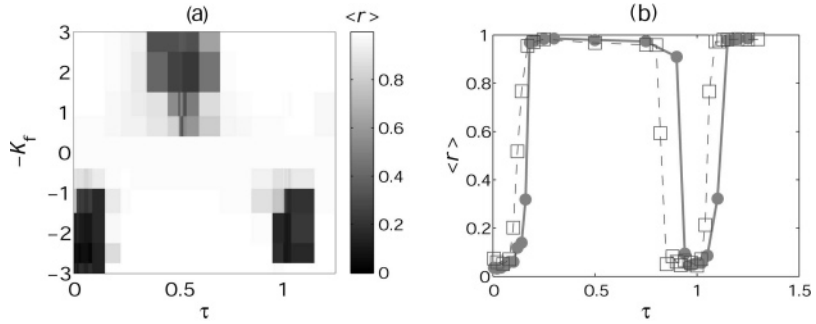

Figure 3. Dependence of the (temporal) mean order $\langle r \rangle$ on the feedback parameters K_f' ($-K_f$) and τ with direct time-delayed feedback of I_{tot} for smooth oscillator populations. The experiment conditions are the same as those given in Figure 2. (a) Grayscale plot of the mean order in the parameter space. (b) Mean order $\langle r \rangle$ vs τ at $K_f' = -2$. Solid circles represent data from the forward scan of τ; open squares represent data from the backward scan of τ.

is used to characterize the degree of synchronization. In this equation, each point in the 2D phase space shown in Figure 2c is treated as a vector $\mathbf{P}_j(t)$; the order is the length of the normalized vector sum. A large value (close to 1) of the order parameter indicates a large extent of synchrony, in which case the population of oscillators behaves as a single, giant oscillator. From the time series of the order in Figure 2d, we can see that a high mean order of $\langle r \rangle = 0.992$ was obtained before the imposition of the feedback and during the delayed feedback the mean order decreased to a very low value of 0.054, which is even lower than that of the uncoupled oscillators (without coupling, the mean order is ~0.15). After the removal of feedback, as resynchronization occurred, the order increased again to a high value of ~1.

To characterize the efficiency of the feedback control, the effects of feedback parameters, feedback gain (K_f'), and time delay (τ) on the order were studied systematically, and the results are summarized in Figure 3. The mean order during the feedback with different values of K_f' and τ is plotted in Figure 3a. There exist multiple "islands" in the parameter space located at $\tau \approx$ constant $+ nT/2$, where effective desynchronization is achieved with the direct time-delayed feedback control (the dark-colored regions in Figure 3a). In other parameter regions, enhanced synchronization is observed. Figure 3a resembles the suppression factor plot shown in Figure 2 of the reported work by Rosenblum and Pikovsky,[19] which shows simulation results of direct feedback control of an ensemble of nonidentical chaotic Rössler oscillators coupled via a mean field. Note that the strongest control occurred at the left lower corner, where $K_f' < 0$ and τ is small (but still nonzero). The effect of desynchronization within each control island decreases with n or the delayed time for direct feedback.

In Figure 3b, the mean order is plotted as a function of τ at a given feedback gain of $K_f' = -2$. There was hysteresis in the mean order as τ was varied in different directions (solid circles for the increase in τ, open squares for the decrease in τ). This bistability of both synchronized and desynchronized states near the boundaries of the desynchronization islands has been predicted in the theoretical studies;[19] these regions are called "weak control" ones, because either a synchronized or desynchronized state can be achieved, depending on the initial conditions.

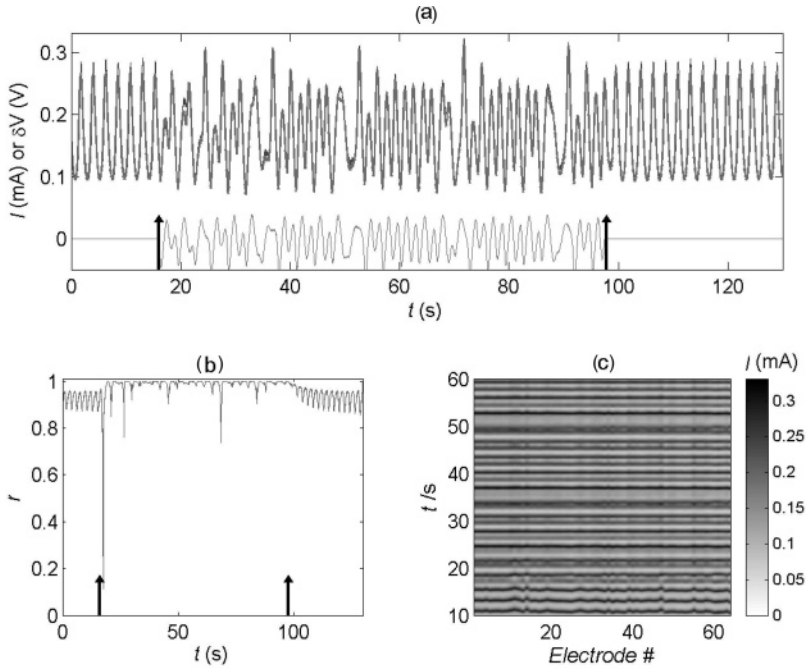

Figure 4. Synchronized irregular behavior of smooth oscillator populations with direct time-delayed feedback of I_{tot} ($K_f' = 7$, $\tau = 0.500$). Other experiment conditions are the same as those given in Figure 2. (a) Time series of mean current (bold line), individual current (thin line), and feedback signal. (b) Time series of order r; $\langle r \rangle$ increased from 0.921 to 0.99, because of the feedback. (c) Grayscale plot of individual currents during the onset of feedback.

With very strong feedback strength, another synchronized state can be obtained, where the periodic oscillatory state of the individual element lost stability and the individual current became irregular. An example of synchronized irregular behavior is presented in Figure 4. As shown in Figure 4a, the mean current (bold line) exhibited irregular oscillations with large amplitudes during the feedback. Because of the high degree of synchronization, the behaviors of the mean and the individual signal were almost identical. The order increased to higher values during the feedback, as a result of the enhanced synchronization (see Figure 4b). Figure 4c shows that all individual oscillations became irregular with feedback.

4.2. Differential Feedback of Total Current. Differential time-delayed feedback of the total current (eq 3) was implemented in experiments for a phase synchronized population of smooth oscillators. Similar to the direct delayed feedback experiments, with differential delayed feedback, we also observed multiple, isolated desynchronization control regions in the parameter plane of the feedback gain and the time delay. Furthermore, we explored the dependence of the control efficiency on the initial degree of synchronization (controlled by coupling strength ϵ), as well as on the feedback parameters.

In Figure 5, the mean order during the feedback obtained with a fixed time delay of $\tau = 0.500$ is plotted as a function of the degree of previous synchronization (described by ϵ) and the feedback gain (K_f'). The grayscale plot of the mean order in the parameter space (see Figure 5a) shows that the feedback shifted the critical coupling for synchronization. Desynchronization can be achieved either by weakening the coupling or by increasing the positive feedback ($K_f' > 0$). Figure 5b better demonstrates how the mean order changes with K_f' at different coupling strengths. Generally, at $\tau = 0.5$, negative feedback ($K_f' < 0$) enhanced the synchronization and positive feedback destroyed it, although there are some exceptions around the transitions for lower coupling strengths. In particular, at $\epsilon = 0.1$ (circles), when the population is phase-synchronized without feedback, only with positive feedback desynchronization is possible. In contrast, when the coupling is lower than the critical value for synchronization ($\epsilon \approx 0.05$), desynchronization can be achieved with weak negative feedback as well as strong positive feedback. The functional relationships between the mean order and the coupling strength at different feedback strengths are presented in Figure 5c. The bold line shows the transition of the order with the coupling only. The solid symbols represent negative feedback cases, and we can see that the transition curve was shifted to higher values with the increase of the strength of the negative feedback. Similarly, the curves with open symbols for the positive feedback show that the transition curve was shifted to lower values with the increase of the strength of the positive feedback. Again, some exceptions are observed near the critical coupling. These results are similar to the simulations results of differential feedback control of an ensemble of globally coupled maps modeling the chaotic bursting of neurons.[19] The deviations from the general trends near the critical coupling in Figures 5b and 5c may be related to the small size of the experimental system.

4.3. Time-Delayed Feedback of the Mean Potential Drop. Similar experimental results were obtained when feedback was applied through the dynamical variable (the mean potential drop, e_{mean}), either with the direct or differential delayed feedback scheme. An example of effective desynchronization achieved with differential delayed feedback of e_{mean} is illustrated in Figure 6.

5. Feedback on Populations of Relaxational Oscillators: Desynchronization and Clustering

Time-delayed feedback experiments were performed with relaxational electrochemical oscillator populations. In sections 5 and 6, only the results of differential feedback through the mean potential drop are presented.

5.1. Desynchronization and Clustering of Weakly Relaxational Oscillators. Time-delayed feedback was first applied to a population of oscillators obtained at a circuit potential of $V_0 = 1.228$ V. At this potential, the oscillation of the individual current is weakly relaxational. With a stronger coupling of $\epsilon =$

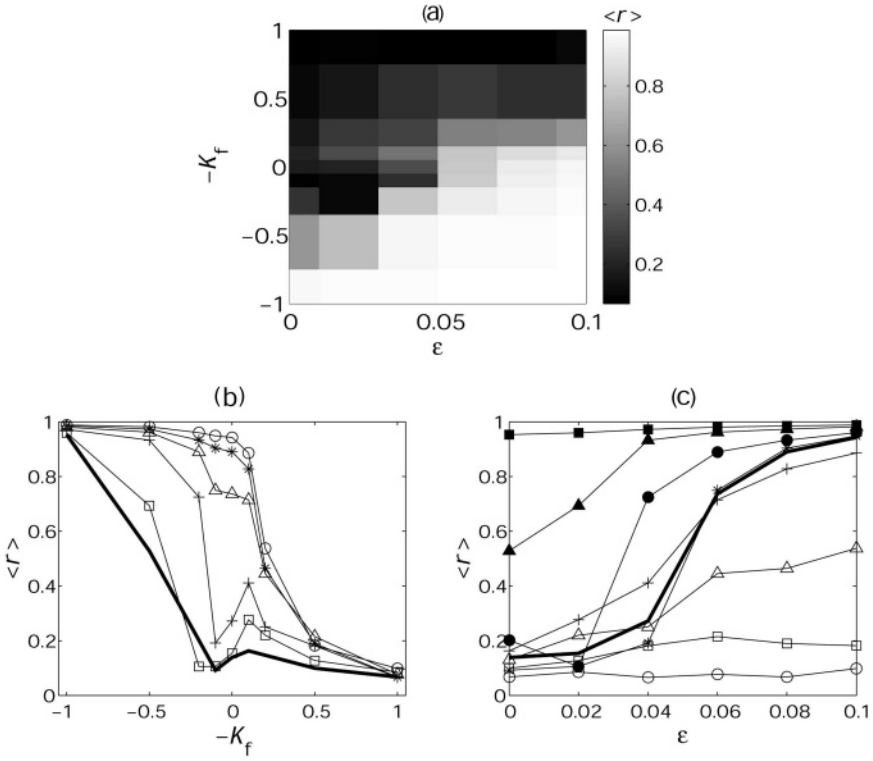

Figure 5. Dependence of mean order $\langle r \rangle$ on feedback strength K_f' ($-K_f$) and coupling strength ϵ at a fixed $\tau = 0.500$ with differential time-delayed feedback of I_{tot}; parameter values are $c = 3$ mol/L, $R_{tot} = 10.2\ \Omega$, and $V_0 = 1.114$ V. (a) Grayscale plot of the mean order in the parameter space. (b) Mean order $\langle r \rangle$ vs K_f': (−) $\epsilon = 0$, (□) $\epsilon = 0.02$, (+) $\epsilon = 0.04$, (△) $\epsilon = 0.06$, (*) $\epsilon = 0.08$, and (○) $\epsilon = 0.1$. (c) Mean order vs ϵ: (○) $K_f' = 1$, (□) $K_f' = 0.5$, (△) $K_f' = 0.2$, (+) $K_f' = 0.1$, (−) $K_f' = 0$, (*) $K_f' = -0.1$, (●) $K_f' = -0.2$, (▲) $K_f' = -0.5$, and (■) $K_f' = -1$.

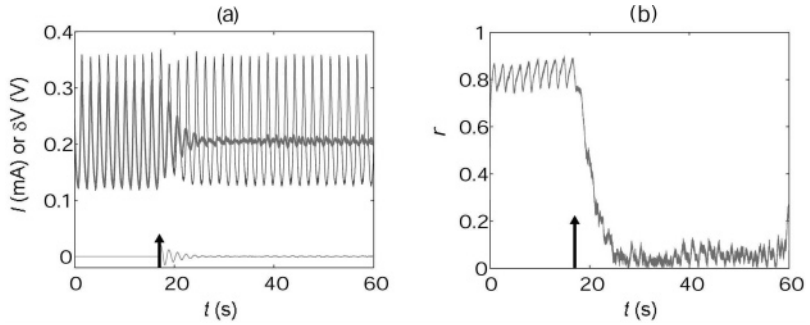

Figure 6. Desynchronization of a population of smooth electrochemical oscillators with a time-delayed differential feedback of e_{mean}; parameter values are $c = 3$ mol/L, $R_{tot} = 10.2\ \Omega$, $V_0 = 1.114$ V, $\epsilon = 0.15$, $K_f' = 2$, $\tau = 0.503$. (a) Time series of mean current (bold line), individual current (thin line), and feedback signal. (b) Time series of order r.

0.3, a highly synchronized state of the mean order $\langle r \rangle = 0.99$ was obtained for the relaxational oscillator population and the period of the mean current was ∼2.2 s.

It is observed that, with proper combinations of the feedback parameters, the cluster of weakly relaxational oscillators can be effectively desynchronized by time-delayed feedback. One particular feature of the application of feedback to a relaxational oscillator population is that the feedback induces and stabilizes multiple clusters as the feedback parameter (for example, τ) changes.

The top row of Figure 7 shows grayscale plots of individual currents before and during feedback experiments with $K_f' = 4$ and various time delays. Without feedback, all elements exhibited almost identical dynamics and oscillated in unison (Figure 7a), which indicates phase synchronization was attained. The time series of the order in Figure 7b shows that the system had a high mean order of 0.99. When feedback was applied with a time delay of $\tau = 0.502$, the cluster broke apart and a two-cluster state emerged (Figure 7c). Note that this is similar to the multibranch entrainment of the population;[37] the elements with low and high intrinsic frequencies form two distinct clusters, while the elements that have intermediate values of intrinsic frequencies can be in either cluster. In the meanwhile, the feedback decreased the order to a mean value of 0.47 with larger variations (Figure 7d). As the time delay was increased to $\tau = 0.558$, the two-cluster state was replaced by a three-cluster one (Figure 7e). The mean order was further decreased to 0.28 with smaller variations (Figure 7f). A further increase of τ to 0.605 leads to a fairly desynchronized state by forming six clusters (Figure 7g), and a very low mean order of $\langle r \rangle = 0.20$ was obtained (Figure 7h). With $\tau = 0.639$ (not shown), a two-cluster state appeared and, thus, the order started to increase again. After the feedback was removed, the population resumed a phase-synchronized state similar to that shown in Figure 7a.

To better illustrate the formation of clusters during the feedback on the relaxational oscillator population, cluster analysis was performed using the same data shown in Figure 7. The results are presented in Figure 8.

Cluster configurations on the array obtained from hierarchical cluster trees are shown in the left column of Figure 8. We can

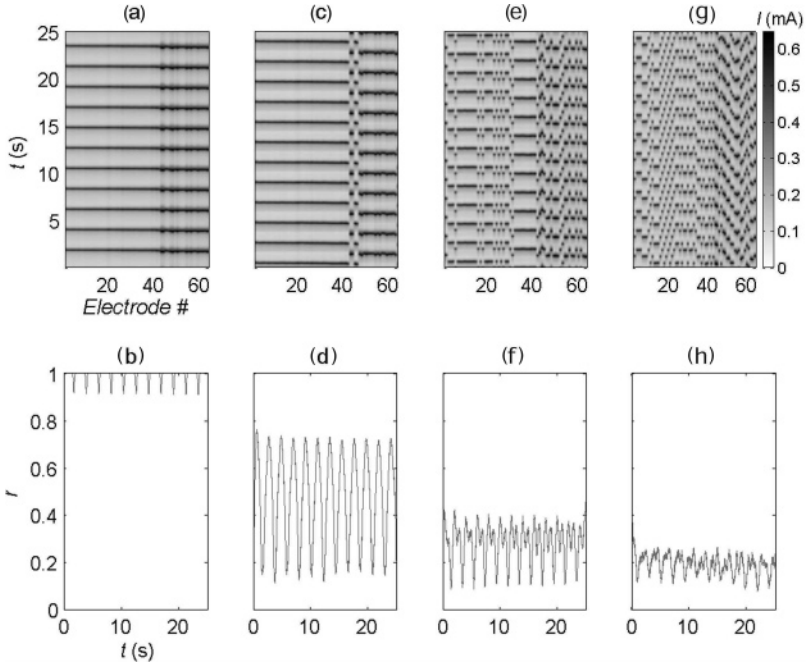

Figure 7. Time-delayed feedback on an ordered population of weakly relaxational oscillators (differential feedback through e_{mean}); parameter values are $c = 3$ mol/L, $R_{tot} = 10.2\ \Omega$, $V_0 = 1.228$ V, and $\epsilon = 0.3$. Top row shows grayscale plots of individual currents (the elements are ordered by their intrinsic frequencies from low to high); the bottom row shows the time-series of order. (a, b) Phase synchronization without feedback; the mean order is $\langle r \rangle = 0.99$. (c, d) Two-cluster state with feedback; the feedback strength is $K_f' = 4$, the time delay was $\tau = 0.502$, and $\langle r \rangle = 0.47$. (e, f) Three-cluster state with $K_f' = 4$, $\tau = 0.558$, and $\langle r \rangle = 0.28$. (g, h) Six-cluster state with $K_f' = 4$, $\tau = 0.605$, and $\langle r \rangle = 0.20$.

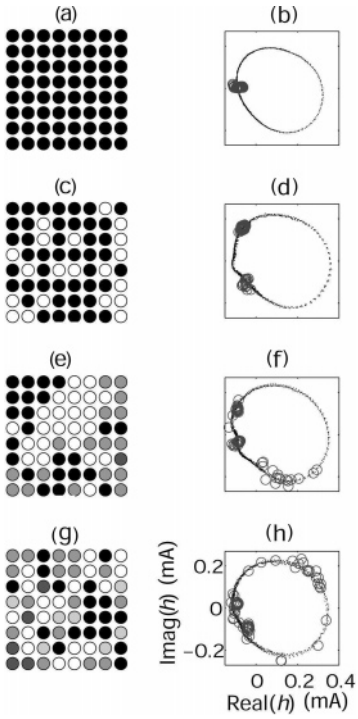

Figure 8. Cluster analysis of data in Figure 7. The left column shows cluster configurations on the array; the right column shows snapshots of the phase points in the 2D phase space. (a, b) Phase synchronization without feedback; $\langle r \rangle = 0.99$. (c, d) Two-cluster state with feedback; $K_f' = 4$, $\tau = 0.502$, and $\langle r \rangle = 0.47$. (e, f) Three-cluster state with feedback of $K_f' = 4$, $\tau = 0.558$, and $\langle r \rangle = 0.28$. (g, h) Six-cluster state with feedback of $K_f' = 4$, $\tau = 0.605$, and $\langle r \rangle = 0.20$.

see that one, two, three, and six clusters were formed before application of the feedback, with the following feedback (K_f') and τ values: for the two-cluster state, $K_f' = 4$ and $\tau = 0.502$; for the three-cluster state, $K_f' = 4$ and $\tau = 0.558$; and for the six-cluster state, $K_f' = 4$ and $\tau = 0.605$. With $\tau = 0.502$, the two-cluster configuration was (42,20) (see Figure 8c). The configuration of the three-cluster state with $\tau = 0.558$ was (24,-23,17) (see Figure 8e), and that of the six-cluster state with $\tau = 0.605$ was (18,18,16,5,4,3) (see Figure 8g). In the snapshots in the phase space (right column of Figure 8), we can see that the single cloud that contains 64 elements before the feedback (Figure 8b) broke apart and formed two (Figure 8d), three (Figure 8f), and more groups (Figure 8h) as feedback was applied with increasing τ within the range of 0.5−0.605. The individual oscillations in each clusters were similar and they remained relaxational periodic during the feedback with slightly deformation on the slow portion, as shown in the right column of Figure 8.

Similar to the feedback on smooth oscillator populations, there are multiple isolated regions of parameters for effective desynchronization control in populations of weakly relaxational oscillators. In other control regions, desynchronization is also achieved by the formation of clusters, but the features of the clustering may be different from those presented in Figures 7 and 8. For example, in the control region, at $\tau \cong 0.2$, more-balanced cluster configurations such as (33,31) for the two-cluster state and (23,21,20) for the three-cluster state were observed. The order variations were much less in more-balanced clustering states.

If $K_f' < 0$, no control regions of effective desynchronization existed for this highly synchronized relaxational oscillator population ($r = 0.99$ with $\epsilon = 0.3$). Instead, synchronization and clustering of irregular individual dynamics were observed with negative feedback.

The occurrence of irregular clustering with a feedback value of $K_f' = -4$ is shown in Figure 9. The grayscale plot of all the individual currents (Figure 9a) shows that the waveforms of all of the elements became quite complicated. The collective dynamics (the mean current) was irregular, with amplitudes that were approximately half of those of the individual one (Figure 9b) and the order was ∼0.5 with large oscillations (Figure 9c). The cluster tree in Figure 9d clearly shows that two main clusters were formed (with one element 'off'). The cluster configuration

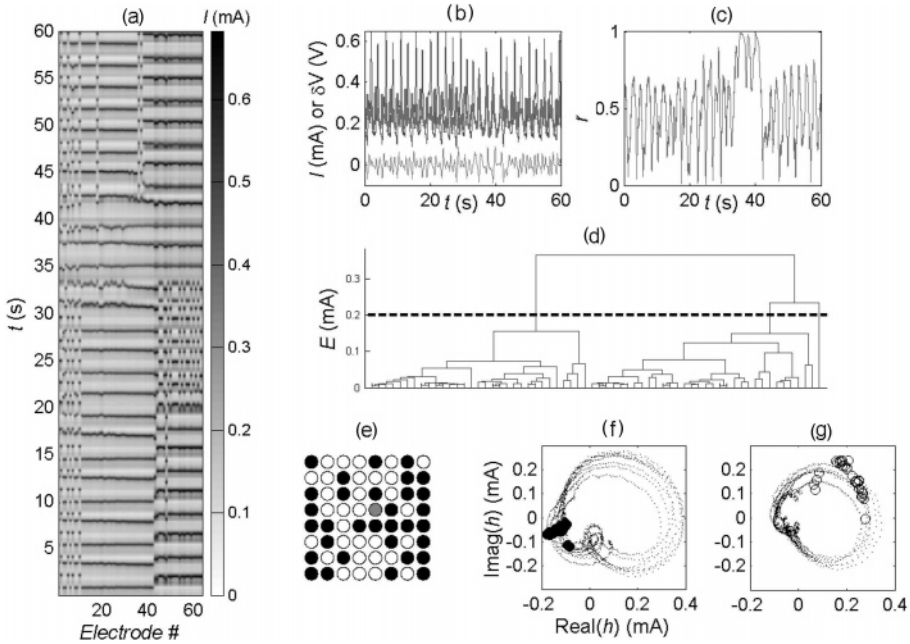

Figure 9. Irregular clusters in the time-delayed feedback experiments on a population of weakly relaxational oscillators; $K_f' = -4$, $\tau = 1.182$. Other experiment conditions are the same as those given in Figure 7. (a) Grayscale plot of individual currents. (b) Time series of mean current (bold line), individual current (thin line), and feedback signal. (c) Time series of order. (d) Cluster trees from time series. (e) Cluster configuration on the array. (f, g) Snapshot of phase points (circles) of the elements that are solid and black (panel f) and are hollow (panel g) in panel e in the 2D phase space at $t = 42.5$ s. Dots represent the trajectory of a typical oscillator in the respective cluster.

was (32,31) (see Figure 9e), where the solid black circles represent the cluster of 32 elements and the hollow circles represent the other cluster. In Figure 9f, the phase points of the elements that are shown as solid black circles in Figure 9e are shown in the 2D phase space at $t = 42.5$ s. A small cloud was formed, because of the clustering. The snapshot of the phase points of the elements forming the other cluster is shown in Figure 9g. The typical trajectory of one element in each cluster is also shown in Figures 9f and 9g, and we can see that the amplitudes of the individual oscillations in the solid black cluster (Figure 9f) are larger than those in the hollow cluster (Figure 9g).

5.2. Cluster Transitions of Strongly Relaxational Oscillators. We then increased the applied potential to $V_0 = 1.273$ V, which is much closer to the saddle-loop bifurcation point of the studied system. The individual oscillation obtained at this potential is strongly relaxational. At $\epsilon = 0.6$, a highly ordered state with $\langle r \rangle = 0.93$ was attained and the mean oscillation had a period of $\sim$2.5 s.

This base state without feedback is presented in Figures 10a and 10b. The grayscale plot of individual currents (Figure 10a) shows two period-2 clusters at $\epsilon = 0.6$. One cluster consisted of elements whose intrinsic frequencies were lower and the other cluster consisted of elements with higher intrinsic frequencies. The oscillations in the cluster of elements with higher intrinsic frequencies were slightly more regular. The order had a high mean value with relatively small variations (see Figure 10b). Through the cluster analysis (Figures 11a−c), we can see that the two clusters were fairly balanced with the configuration of (38,26). Figures 11b and 11c show that the elements within each cluster moved as one entity along the typical trajectory of a single oscillator in the respective cluster; however, the local dynamics different from one cluster to another.

When time-delayed feedback is applied to this system, the order cannot be sufficiently decreased; thus, no effective desynchronization can be achieved. Nevertheless, it is observed that stable new clustering states with different cluster configurations can be obtained with time-delayed feedback.

Figures 10c and 10d show that, with a feedback value of $K_f' = -3$ and $\tau = 1.195$, irregular clusters were induced in the coupled strongly relaxational oscillators. All individual currents oscillated irregularly, as shown in Figure 10c. The order exhibited larger oscillations, because of the feedback, and its mean value decreased somewhat (see Figure 10d). The cluster analysis shows that there were two clusters with a configuration of (44,20) with this feedback (see Figure 11d). In comparison with the cluster configuration before the feedback application (Figure 11a), the new cluster state obtained with the feedback was quite unbalanced as the old, slightly larger cluster absorbed more elements from the old smaller one. Within each cluster, the dynamics of the elements were similar and irregular, but the irregular oscillations in one cluster were different from those in the other cluster, as shown in Figures 11e and 11f. Thus, the feedback not only produced an unbalanced two-cluster state but also considerably changed the individual dynamics.

With an increase in the feedback gain to $K_f' = -4$, a new periodic two-cluster state was obtained, as illustrated in Figure 10e. The order oscillated in large amplitudes with the stronger feedback strength (see Figure 10f). The two clusters were very unbalanced with a configuration of (21,43) (see Figure 11g). Different from the previous case with a weaker feedback gain of $K_f' = -3$ (Figure 11d), the old larger cluster (indicated by black circles in Figure 11a) gave almost half of its elements away to the other cluster and became the minor one, with only 21 elements left. The oscillations in both clusters were periodic with higher periodicity; larger amplitudes in the smaller cluster (Figure 11h) and smaller amplitudes in the larger cluster (Figure 11i) were observed.

After the removal of the feedback of $K_f' = -4$ and $\tau = 1.195$, a highly unbalanced two-cluster state of the coupled strongly relaxational oscillators was obtained as shown in Figure 10g. The collective behavior, the cluster configuration, and the individual dynamics all were changed some time after the feedback application. A comparison of Figure 10h with Figure 10b shows that the collective behavior or the evolution of the order of the population exhibited large oscillations with a lower

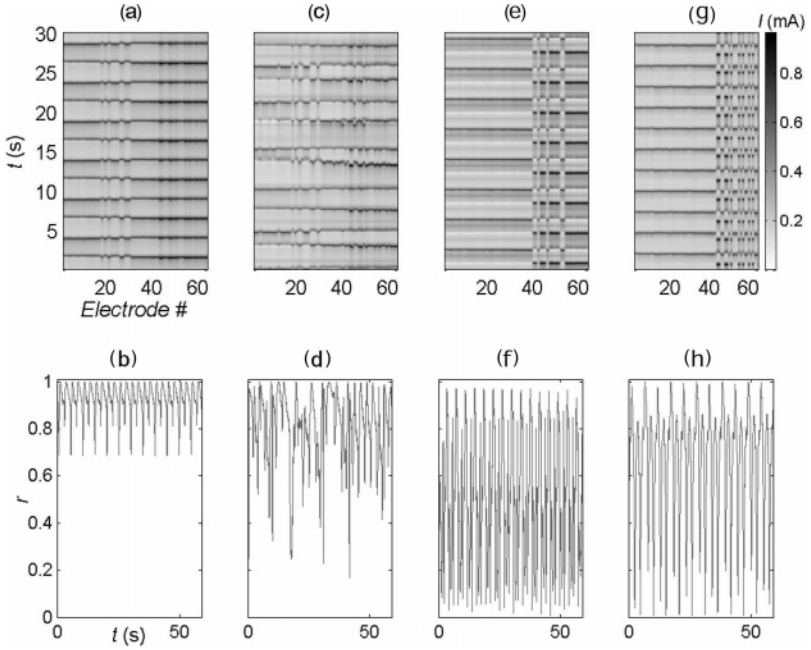

Figure 10. Time-delayed feedback on an ordered population of strongly relaxational oscillators; parameter values are $c = 3$ mol/L, $R_{tot} = 10.2\ \Omega$, $V_0 = 1.273$ V, and $\epsilon = 0.6$. The top row shows a grayscale plot of individual currents; the bottom row shows the time-series of order. (a, b) Balanced periodic two-cluster state before turn-on of the feedback. (c, d) Balanced irregular clusters with a feedback strength of $K_f' = -3$ and a time delay of $\tau = 1.195$. (e, f) Unbalanced two-cluster state with $K_f' = -4$ and $\tau = 1.195$. (g, h) Another unbalanced two-cluster state obtained after removal of the feedback.

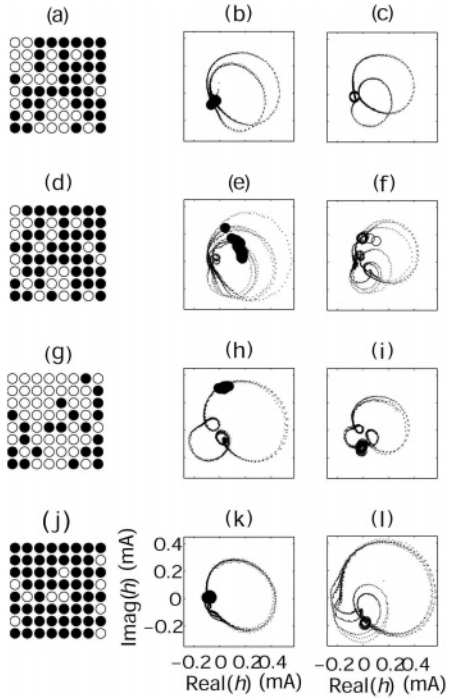

Figure 11. Cluster analysis of the data in Figure 10. The left column shows cluster configurations on the array; the middle column shows snapshots of the phase points (circles) of the elements that are solid and black in the configuration plot (dots represent the trajectory of a typical oscillator in the respective cluster); and the right column shows snapshots of the phase points of the elements that are hollow in the configuration plot and a typical trajectory in this cluster. (a−c) Balanced periodic two-cluster state before turn-on of the feedback. (d−f) Balanced irregular clusters with a feedback strength of $K_f' = -3$ and a time delay of $\tau = 1.195$. (g−i) Unbalanced two-cluster state with $K_f' = -4$ and $\tau = 1.195$. (j−l) Another unbalanced two-cluster state obtained after removal of the feedback.

mean value. The new cluster state had a configuration of (54,-10) (see Figure 11j), in contrast with (38,36) obtained before the feedback (Figure 11a). The individual oscillations within each cluster became more different; those in the bigger cluster had smaller amplitudes (Figure 11k), whereas those in the smaller cluster had larger amplitudes (Figure 11l).

6. Feedback on Populations of Chaotic Oscillators: Desynchronization, Amplitude Death, and Enhanced Synchronization

We also performed feedback experiments on a population of 64 chaotic electrochemical oscillators obtained at $V_0 = 1.333$ V in a 4.5 mol/L electrolyte with a total resistance of 14.2 Ω.

The behavior of a single chaotic oscillator is shown in Figure 12a. The oscillation was low-dimensional chaotic with an information dimension of 2.3[38] and was phase coherent.[39] Phase synchronization was achieved by adding a coupling of strength $\epsilon = 0.3$. An ordered state can be seen in the spatiotemporal plot of the individual currents (see Figure 12b). We calculated the Hilbert phase using the time-series data in a manner similar to that for periodic oscillators. The average period of the collective oscillation was 0.8 s.

With a delayed feedback of $K_f' = 3.5$ and $\tau = 0.125$, desynchronization was achieved as illustrated in Figure 13a. The time-series plot of the currents show that the mean current gradually reached an almost-stationary state after the feedback was turned on, while the individual current remained oscillatory. Note that the oscillation of the individual element became periodic during the feedback, which may be due to the fact that the oscillator is only weakly chaotic and phase coherent. (Several elements actually attained steady states when the majority of the population became periodic and desynchronized. These elements were closer to their Hopf bifurcation points; their amplitudes without feedback were relatively smaller, in comparison to those of others.)

With a longer time delay of $\tau = 0.208$, amplitude death was observed in the chaotic oscillator population, as shown in Figure 13b. Both the collective and the individual signal went to and was maintained in steady states during the feedback. The closeness of the applied potential to Hopf bifurcation points

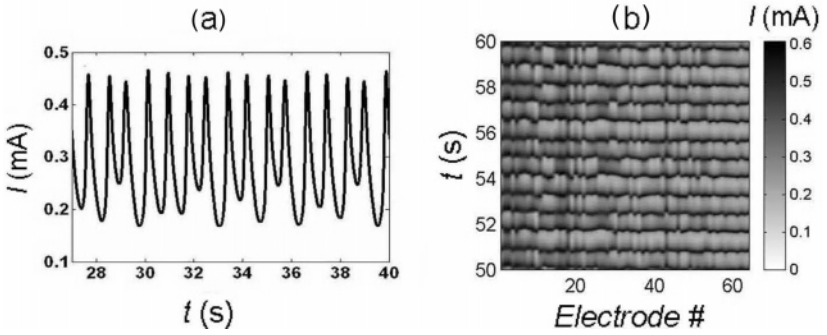

Figure 12. Phase synchronization of 64 coupled chaotic electrochemical oscillators; parameter values are $c = 4.5$ mol/L, $R_{tot} = 14.2\ \Omega$, $V_0 = 1.333$ V, and $\epsilon = 0.3$. (a) Time series of a single oscillator. (b) Grayscale plot of all individual currents.

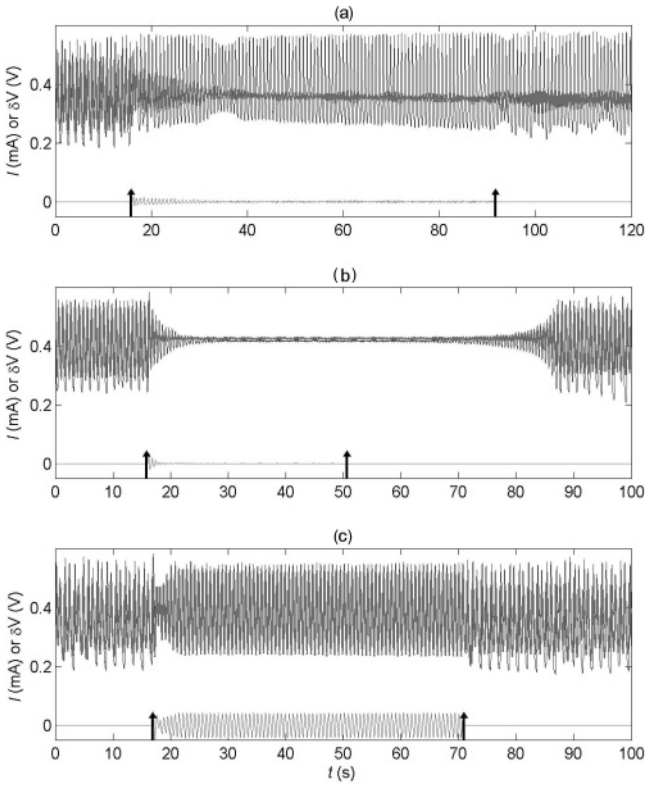

Figure 13. Time series of mean current (bold line), individual current (thin line), and feedback signal in feedback experiments on a phase-synchronized population of chaotic oscillators (differential feedback of e_{mean}): (a) desynchronization with $K'_f = 3.5$ and $\tau = 0.125$ (before feedback, $\langle r \rangle = 0.80$; during feedback, $\langle r \rangle = 0.08$); (b) amplitude death with $K'_f = 3.5$ and $\tau = 0.208$; (c) enhanced phase synchronization with local period dynamics at $K'_f = 3.5$ and $\tau = 0.525$ (before feedback, $\langle r \rangle = 0.80$; during feedback, $\langle r \rangle = 0.93$).

may account for the occurrence of amplitude death with feedback in the experiments of coupled chaotic electrochemical oscillators.

When the time delay is set even higher (for example, with $\tau = 0.525$), enhanced phase synchronization of the oscillator population was attained (see Figure 13). The mean current almost overlapped with the individual signal, because of the high degree of synchronization. Again, the individual dynamics became periodic during the feedback.

7. Optimization of Feedback Parameters, Using a Phase Model Approach

The success of the linear feedback method is dependent on the proper adjustment of the feedback parameters (the gain and the delay). Although general statements about the proper adjustment of these parameters for a specific system are difficult to obtain, phase models can be used to optimize feedback parameters for application to experiments with populations of oscillators.

The collective effect weak inherent coupling and feedback in an oscillator population can be described by a phase model:[40−42]

$$\frac{d\phi_i}{dt} = \omega_i + \sum_{j=1}^{N} \bar{H}(\phi_j - \phi_i) \qquad (13)$$

where ϕ_i and ω_i are the phase and the natural frequency of the ith oscillator, respectively. $\bar{H}(\Delta\phi)$ is an overall interaction function that describes the combined effect of feedback and coupling:

$$\bar{H}(\Delta\phi) = KH_c(\Delta\phi) + K'H_{f,\tau}(\Delta\phi)$$

where $H_c(\Delta\phi)$ is the interaction function for coupling and $H_{f,\tau}(\Delta\phi)$ is the interaction functions for the feedback with τ delay; K is the coupling strength and K' is the feedback gain. The interaction functions for coupling can be determined from the oscillator waveform [$e(\phi)$] and the response function [$Z(\phi)$]:[40,41]

$$H_c(\Delta\phi) = \frac{1}{2\pi}\int_{\phi=0}^{2\pi} Z(\phi)\left[\frac{e(\phi+\Delta\phi) - e(\phi)}{2}\right] d\phi$$

The interaction function for feedback should also consider the feedback delay:[43]

$$H_{f,\tau}(\Delta\phi) = \frac{1}{2\pi}\int_{\phi=0}^{2\pi} Z(\phi)\left[\frac{e(\phi+\Delta\phi-\tau) + e(\phi-\tau)}{2}\right] d\phi$$

The oscillator waveform and the response function has been previously obtained in independent experiments for the smooth oscillators;[42] therefore, the overall interaction function $\bar{H}(\Delta\phi)$ can be readily calculated for various K, K', and τ values. The stability of the synchronized state can be characterized by the eigenvalue[44,45] of the one-cluster solution of the homogeneous system ($\omega_i = \omega$) in eq 13:

$$\lambda = \frac{d\bar{H}(\Delta\phi)}{d\Delta\phi}$$

Figure 14 shows the eigenvalues in the K' vs τ parameter space for the smooth oscillators at $K = 1$. The diagram was obtained using a response function and an oscillation waveform from a single oscillator and did not require experiments with a

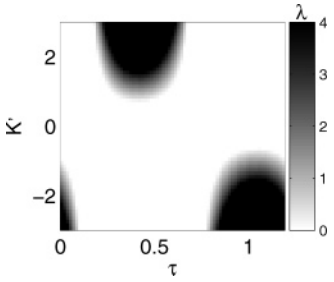

Figure 14. Desynchronization islands in a phase model obtained for a globally coupled smooth oscillators with linear feedback. The eigenvalue of the one-cluster state obtained from the phase model (constructed from experiments on a single oscillator) is shown in the K' vs τ parameter space at $K = 1$.

population; nevertheless, it can quantitatively reproduce the three desynchronization islands that occur with delays of ~ 0, π, and 2π.

8. Concluding Remarks

Control of collective dynamics with global time-delayed feedback has been experimentally studied in populations of electrochemical oscillators. We implemented direct and differential delayed feedback to (phase) synchronized smooth, relaxational, and chaotic electrochemical oscillator populations. Effects of feedback gain and time delay on the collective behavior of the populations were systematically studied. We performed the experiments using 64 oscillators; as we have shown previously,[39] this is a sufficiently large number to obtain the statistical features of collective dynamics of a population of oscillators. The geometry of the elements has a minor role, because of the very weak local coupling, which is due to mass transfer under the conditions of these experiments.

It has been shown that effective desynchronization can be achieved with direct and differential feedback of time-delayed dynamical (e_{mean}) or measurable (I_{tot}) variables in oscillator populations. Multiple isolated desynchronization control regions located at $\tau \approx$ constant $+ nT/2$ are found in the feedback experiments with both control strategies. The strongest control region is obtained with $n = 0$ and the desynchronization effect decreases with n. The oscillation of the mean current (the collective signal) almost vanishes within the strong control region, while all the individual elements maintain periodic oscillations. The feedback signal becomes very small when desynchronization is effectively achieved; however, this small quantity is necessary for stabilizing the steady state of the collective signal. Near the boundaries of each control region, there are "weak control" regions where either s synchronized or desynchronized state can be stable, depending on the initial conditions. With very strong feedback strength, the individual limit cycles lose stability and a synchronized irregular state is observed.

It is found that, at a given time delay, the change in the feedback gain can shift the critical coupling for synchronization. For example, at $\tau = 0.5$, generally, negative feedback ($K_f' < 0$) enhances the synchronization and positive feedback destroys it; correspondingly, the critical coupling becomes smaller with a negative gain and larger with a positive gain.

In particular, we observed that clustering accompanies the occurrence of desynchronization in time-delayed feedback of oscillator populations that contain elements that are weakly relaxational. The original cluster breaks apart with feedback and more and more clusters form while the feedback parameters are adjusted toward the control region. The clusters can be more or less balanced, depending on feedback parameters. Less fluctuations of the order are observed in balanced cluster states. Stable irregular clusters can also be induced with time-delayed feedback in a weakly relaxational oscillator population.

When the oscillators are strongly relaxational, the one-cluster state is no longer stable with coupling: only a two-cluster state of the population is observed. There are multiple cluster configurations in this system. The global time-delayed feedback cannot effectively decrease the order. Instead, the feedback can change both the cluster configurations and the individual dynamics; (highly) unbalanced two-cluster states with irregular or multiperiodic local oscillations have been observed.

Although the linear time-delayed feedback seems to be effective in the destruction of the one-cluster state, the experimental results imply that a more powerful methodology is required for relaxational oscillators that exhibit clustering. In such scenarios, a nonlinear feedback can be used to obtain efficient desynchronization;[43] a methodological approach has been developed to obtain optimal nonlinear feedback parameters with which cluster states can be destroyed.

The application of global time-delayed feedback to a phase-synchronized chaotic oscillator population can also successfully suppress the collective oscillations. This can be achieved either through desynchronization or through amplitude death. At a given feedback strength, desynchronization, amplitude death, and enhanced synchronization occurs with a low, intermediate, and high value of the time delay, respectively. During desynchronization and enhanced synchronization, the feedback also changes the individual oscillations from chaotic to periodic.

Time-delay induced amplitude death has been predicted in theoretical studies of coupled oscillators[46,47] and observed in experiments of two time-delayed coupled oscillators.[48] The effect of linear and nonlinear time-delayed feedback on the dynamics (including amplitude death) of a single Hopf bifurcation oscillator has been numerically and analytically investigated, in an attempt to understand the collective behavior of a large number of coupled limit cycle oscillators.[49] The amplitude death with global time-delayed feedback in the chaotic electrochemical oscillator population provides experimental evidence of amplitude death in a oscillator population, which, to date, has been very limited. The observed amplitude death may be related to the fact that the oscillators are close to their Hopf bifurcation points; previously, with the same nickel−sulfuric acid electrochemical system, amplitude death has been observed in two coupled oscillators that are close to their Hopf bifurcations.[50]

Experimental studies on linear global time-delayed feedback to synchronized electrochemical oscillator populations have provided laboratory evidence to the findings in the theoretical studies;[19,20] bounded regions of desynchronization in the parameter plane, hysteresis phenomenon around the boundaries, synchronization of chaotic behavior with very strong feedback strength, and shift of the synchronization transition curves were all reproduced in the experiments. Using time-delayed feedback to achieve desynchronization is more convenient and more effective, in comparison to desynchronization by decrease of coupling[41,51] and by pulse stimuli.[52,53] Further work on feedback for desynchronization can focus on nonlinear feedback[24] or localized feedback,[24] which have exhibited a more robust control.

The destruction of the highly ordered one-cluster state to a desynchronized state can have a significant effect on system performance. For the evaluation of the system performance, one would consider the qualitative dynamic features of the mean signal: in our example, the mean current or mean potential.

When the system is in a synchronized one-cluster state, the mean signal is strongly oscillatory, with a characteristic period; however, when desynchronization occurs, the resulting collective signal is approximately constant with statistical fluctuations around a mean value. Therefore, the proposed feedback method could be used in applications when elimination of a rhythmic global signal is desirable with weak feedback signals that do not suppress local oscillations. An example of such an application is the suppression of tremors or seizures where the pathological neuronal synchronization should be suppressed but the total elimination of neuronal spiking could be too drastic.[15]

Acknowledgment

We thank Bruce Nauman for his stimulating studies in the field of chemical engineering science and practice. This work was supported in part by the National Science Foundation (NSF).

Literature Cited

(1) Ottino, J. M. Complex systems. *AIChE J.* **2003**, *49* (2), 292.

(2) Ertl, G. Oscillatory kinetics and spatio-temporal self-organization in reactions at solid surfaces. *Science* **1991**, *254*, 1750.

(3) Steinbock, O.; Zykov, V.; Muller, S. C. Control of spiral-wave dynamics in active media by periodic modulation of excitability. *Nature* **1993**, *366* (6453), 322.

(4) Mikhailov, A. S.; Showalter, K. Control of waves, patterns and turbulence in chemical systems. *Phys. Rep.* **2006**, *425* (2−3), 79.

(5) Sakurai, T.; Mihaliuk, E.; Chirila, F.; Showalter, K. Design and control of wave propagation patterns in excitable media. *Science* **2002**, *296* (5575), 2009.

(6) Shvartsman, S. Y.; Schutz, E.; Imbihl, R.; Kevrekidis, I. G. Dynamics of catalytic reactions on microdesigned surfaces. *Catal. Today* **2001**, *70* (4), 301.

(7) Petrov, V.; Ouyang, Q.; Swinney, H. L. Resonant pattern formation in a chemical system. *Nature* **1997**, *388* (6643), 655.

(8) Wolff, J.; Papathanasiou, A. G.; Kevrekidis, I. G.; Rotermund, H. H.; Ertl, G. Spatiotemporal addressing of surface activity. *Science* **2001**, *294* (5540), 134.

(9) Alonso, S.; Sagues, F.; Mikhailov, A. S. Taming Winfree turbulence of scroll waves in excitable media. *Science* **2003**, *299* (5613), 1722.

(10) Schlesner, J.; Zykov, V.; Engel, H.; Schoell, E.; Stabilization of unstable rigid rotation of spiral waves in excitable media. *Phys. Rev. E* **2006**, *74*, 046215.

(11) Kim, M.; Bertram, M.; Pollmann, M.; von Oertzen, A.; Mikhailov, A. S.; Rotermund, H. H.; Ertl, G. Controlling chemical turbulence by global delayed feedback: Pattern formation in catalytic co oxidation on Pt(110). *Science* **2001**, *292* (5520), 1357.

(12) Marwaha, G.; Luss, D. Formation and dynamics of a hot zone in radial flow reactor. *AIChE J.* **2002**, *48* (3), 617.

(13) Graham, M. D.; Lane, S. L.; Luss, D. Temperature pulse dynamics on a catalytic ring. *J. Phys. Chem.* **1993**, *97* (29), 7564.

(14) Braune, M.; Engel, H. Compound rotation of spiral waves in a light-sensitive Belousov−Zhabotinsky medium. *Chem. Phys. Lett.* **1993**, *204* (3−4), 257.

(15) Tass, P. A. *Phase Resetting in Medicine and Biology. Stochastic Modeling and Data Analysis*; Springer: Berlin, 1999.

(16) Pikovsky, A. S.; Rosenblum, M. G.; Kurths, J. *Synchronization: A Universal Concept in Nonlinear Science*; Univeristy Press: Cambridge, U.K., 2001.

(17) Manrubia, S. C.; Mikhailov, A. S.; Zanette, D. H. *Emergence of Dynamical Order: Synchronization Phenomena in Complex Systems*; World Scientific: Singapore, 2004.

(18) Epstein, I. R.; Pojman, J. A. *An Introduction to Nonlinear Chemical Dynamics: Oscillations, Waves, Patterns, and Chaos*; Oxford University Press: New York, 1998.

(19) Rosenblum, M. G.; Pikovsky, A. S. Controlling synchronization in an ensemble of globally coupled oscillators. *Phys. Rev. Lett.* **2004**, *92* (11), 114102.

(20) Rosenblum, M.; Pikovsky, A. Delayed feedback control of collective synchrony: An approach to suppression of pathological brain rhythms. *Phys. Rev. E* **2004**, *70* (4), 041904.

(21) Battogtokh, D.; Mikhailov, A. Controlling turbulence in the complex Ginzburg−Landau equation. *Physica D* **1996**, *90* (1−2), 84.

(22) Parmananda, P.; Hildebrand, M.; Eiswirth, M. Controlling turbulence in coupled map lattice systems using feedback techniques. *Phys. Rev. E* **1997**, *56* (1), 239.

(23) Bertram, M.; Mikhailov, A. S. Pattern formation in a surface chemical reaction with global delayed feedback. *Phys. Rev. E* **2001**, *63* (6), 066102.

(24) Hauptmann, C.; Popovych, O. V.; Tass, P. A. Delayed feedback control of synchronization in locally coupled neuronal networks. *Neurocomputing* **2005**, *65*, 759.

(25) Popovych, O. V.; Hauptmann, C.; Tass, P. A. Effective desynchronization by nonlinear delayed feedback. *Phys. Rev. Lett.* **2005**, *94*, 164102.

(26) Vanag, V. K.; Yang, L. F.; Dolnik, M.; Zhabotinsky, A. M.; Epstein, I. R. Oscillatory cluster patterns in a homogeneous chemical system with global feedback. *Nature* **2000**, *406*, 389.

(27) Wang, W.; Kiss, I. Z.; Hudson, J. L. Clustering of arrays of chaotic chemical oscillators by feedback and forcing. *Phys. Rev. Lett.* **2001**, *86*, 4954.

(28) Wang, W.; Kiss, I. Z.; Hudson, J. L. Synchronization and clustering of arrays of electrochemical oscillators with global feedback. *Ind. Eng. Chem. Res.* **2002**, *41*, 330.

(29) Wang, W. Synchronization and Clustering of Arrays of Electrochemical Oscillators, Ph.D. Dissertation, Department of Chemical Engineering, University of Virginia, Charlottesville, VA, May 2001.

(30) Kiss, I. Z.; Wang, W.; Hudson, J. L. Experiments on arrays of globally coupled periodic electrochemical oscillators. *J. Phys. Chem. B* **1999**, *103*, 11433.

(31) Wang, W.; Kiss, I. Z.; Hudson, J. L. Experiments on arrays of globally coupled chaotic electrochemical oscillators: Synchronization and clustering. *Chaos* **2000**, *10*, 248.

(32) Zhai, Y. M.; Kiss, I. Z.; Daido, H.; Hudson, J. L. Extracting order parameters from global measurements with application to coupled electrochemical oscillators. *Physica D* **2004**, *199* (3−4), 387.

(33) Haim, D.; Lev, O.; Pismen, L. M.; Sheintuch, M. Modeling periodic and chaotic dynamics in anodic nickel dissolution. *J. Phys. Chem.* **1992**, *96*, 2676.

(34) Zhai, Y. M.; Kiss, I. Z.; Hudson, J. L. Emerging coherence of oscillating chemical reactions on arrays: Experiments and simulations. *Ind. Eng. Chem. Res.* **2004**, *43*, 315.

(35) Pikovsky, A. S.; Rosenblum, M. G.; Osipov, G. V.; Kurths, J. Phase synchronization of chaotic oscillators by external driving. *Physica D* **1997**, *104*, 219.

(36) Kiss, I. Z.; Zhai, Y. M.; Hudson, J. L. Emerging coherence in a population of chemical oscillators. *Science* **2002**, *296*, 1676.

(37) Daido, H. Multibranch entrainment and scaling in large populations of coupled oscillators. *Phys. Rev. Lett.* **1996**, *77* (7), 1406.

(38) Kiss, I. Z.; Wang, W.; Hudson, J. L. Complexity of globally coupled chaotic electrochemical oscillators. *Phys. Chem. Chem. Phys.* **2000**, *2*, 3847.

(39) Kiss, I. Z.; Zhai, Y.; Hudson, J. L. Collective dynamics of chaotic chemical oscillators and the law of large numbers. *Phys. Rev. Lett.* **2002**, *88*, 238301.

(40) Winfree, A. T. *The Geometry of Biological Time*; Springer−Verlag: New York, 1980.

(41) Kuramoto, Y. *Chemical Oscillations, Waves, and Turbulence*; Springer−Verlag: Berlin, 1984.

(42) Kiss, I. Z.; Zhai, Y.; Hudson, J. L. Predicting mutual entrainment of oscillators with experimental-based phase models. *Phys. Rev. Lett.* **2005**, *94*, 248301.

(43) . Kiss, I. Z.; Rusin, G. C.; Kori, H.; Hudson, J. L. Engineering complex dynamical structures: Sequential patterns and desynchronization. *Science* **2007**, *316*, 1140858.

(44) Okuda, K. Variety and generality of clustering in globally coupled oscillators. *Physica D* **1993**, *63* (3−4), 424.

(45) Golomb, D.; Hansel, D.; Shraiman, B.; Sompolinsky, H. Clustering in globally coupled phase oscillators. *Phys. Rev. A* **1992**, *45* (6), 3516.

(46) Reddy, D. V. R.; Sen, A.; Johnston, G. L. Time delay induced death in coupled limit cycle oscillators. *Phys. Rev. Lett.* **1998**, *80* (23), 5109.

(47) Reddy, D. V. R.; Sen, A.; Johnston, G. L. Time delay effects on coupled limit cycle oscillators at hopf bifurcation. *Phys. D* **1999**, *129* (1−2), 15.

(48) Reddy, D. V. R.; Sen, A.; Johnston, G. L. Experimental evidence of time-delay-induced death in coupled limit-cycle oscillators. *Phys. Rev. Lett.* **2000**, *85* (16), 3381−3384.

(49) Reddy, D. V. R.; Sen, A.; Johnston, G. L. Dynamics of a limit cycle oscillator under time delayed linear and nonlinear feedbacks. *Physica D* **2000**, *144* (3−4), 335.

(50) Zhai, Y. M.; Kiss, I. Z.; Hudson, J. L. Amplitude death through a Hopf bifurcation in coupled electrochemical oscillators: Experiments and simulations. *Phys. Rev. E* **2004**, *69* (2), 026208.

(51) Maistrenko, Y.; Popovych, O.; Burylko, O.; Tass, P. A. Mechanism of desynchronization in the finite-dimensional kuramoto model. *Phys. Rev. Lett.* **2004**, *93* (8), 084102.

(52) Tass, P. A. Effective desynchronization by means of double-pulse phase resetting. *Europhys. Lett.* **2001**, *53* (1), 15.

(53) Tass, P. A. A model of desynchronizing deep brain stimulation with a demand-controlled coordinated reset of neural subpopulations. *Biol. Cybern.* **2003**, *89* (2), 81.

Received for review June 22, 2007
Revised manuscript received October 2, 2007
Accepted October 4, 2007

IE0708632